

## Identification of the skeletal progenitor cells forming osteophytes in osteoarthritis

Anke J. Roelofs<sup>1\*</sup>, Karolina Kania<sup>1\*</sup>, Alexandra J. Rafipay<sup>1</sup>, Meike Sambale<sup>2</sup>, Stephanie T. Kuwahara<sup>3</sup>, Fraser Collins<sup>1</sup>, Joanna Smeeton<sup>3,4</sup>, Maxwell A. Serowoky<sup>3</sup>, Lynn Rowley<sup>5</sup>, Hui Wang<sup>1</sup>, René Gronewold<sup>2</sup>, Chrysa Kapeni<sup>6</sup>, Simón Méndez-Ferrer<sup>6</sup>, Christopher B. Little<sup>7</sup>, John F. Bateman<sup>5</sup>, Thomas Pap<sup>2</sup>, Francesca V. Mariani<sup>3</sup>, Joanna Sherwood<sup>2</sup>, J. Gage Crump<sup>3,8</sup>, Cosimo De Bari<sup>1,8</sup>

<sup>1</sup> Arthritis and Regenerative Medicine Laboratory, Aberdeen Centre for Arthritis and Musculoskeletal Health, Institute of Medical Sciences, University of Aberdeen, Aberdeen AB25 2ZD, UK;

<sup>2</sup> Institute of Musculoskeletal Medicine, University Hospital Münster, Münster D-48149, Germany;

<sup>3</sup> Eli and Edythe Broad CIRM Center for Regenerative Medicine and Stem Cell Research, Department of Stem Cell Biology and Regenerative Medicine, Keck School of Medicine, University of Southern California, Los Angeles, CA 90033, USA;

<sup>4</sup> Department of Rehabilitation and Regenerative Medicine, Columbia University Irving Medical Center, Columbia University, New York, NY 10032, USA;

<sup>5</sup> Murdoch Children's Research Institute, Department of Paediatrics, University of Melbourne, Parkville, Victoria 3052, Australia;

<sup>6</sup> Wellcome Trust-Medical Research Council Cambridge Stem Cell Institute and Department of Haematology, University of Cambridge, and NHS Blood and Transplant, Cambridge CB2 0AW, UK;

<sup>7</sup> Raymond Purves Bone and Joint Research Laboratories, Royal North Shore Hospital, Kolling Institute and Institute of Bone and Joint Research, University of Sydney, Sydney, Australia;

\* Equal contribution;

<sup>8</sup> Co-Corresponding Authors: Cosimo De Bari, institute of Medical Sciences, Foresterhill, Aberdeen AB25 2ZD, UK, c.debari@abdn.ac.uk; Gage Crump, Eli and Edythe Broad CIRM Center for Regenerative Medicine and Stem Cell Research at USC, 1425 San Pablo Street, BCC 406 Los Angeles, CA 90033-9080, gcrump@med.usc.edu.

Word count: 2,997

## ABSTRACT

**Objectives.** Osteophytes are highly prevalent in osteoarthritis (OA) and are associated with pain and functional disability. These pathological outgrowths of cartilage and bone typically form at the junction of articular cartilage, periosteum and synovium. The aim of this study was to identify the cells forming osteophytes in OA.

**Methods.** Fluorescent genetic cell-labelling and tracing mouse models were induced with tamoxifen to switch on reporter expression, as appropriate, followed by surgery to induce destabilization of the medial meniscus (DMM). Contributions of fluorescently labelled cells to osteophytes after 2 or 8 weeks, and their molecular identity, were analysed by histology, immunofluorescence staining, and *in situ* hybridisation. *Pdgfra-H2BGFP* mice and *Pdgfra-CreER* mice crossed with multi-colour *Confetti* reporter mice were used for identification and clonal tracing of mesenchymal progenitors. Mice carrying *Col2-CreER*, *Nes-CreER*, *LepR-Cre*, *Grem1-CreER*, *Gdf5-Cre*, *Sox9-CreER* or *Prg4-CreER* were crossed with tdTomato reporter mice to lineage-trace chondrocytes and stem/progenitor cell sub-populations.

**Results.** Articular chondrocytes or skeletal stem cells identified by *Nes*, *LepR*, or *Grem1* expression did not give rise to osteophytes. Instead, osteophytes derived from *Pdgfra*-expressing stem/progenitor cells in periosteum and synovium that are descendants from the *Gdf5*-expressing embryonic joint interzone. Further, we show that *Sox9*-expressing progenitors in periosteum supplied hybrid skeletal cells to the early osteophyte, while *Prg4*-expressing progenitors from synovial lining contributed to cartilage capping the osteophyte, but not to bone.

**Conclusion.** Our findings reveal distinct periosteal and synovial skeletal progenitors that cooperate to form osteophytes in OA. These cell populations could be targeted in disease modification for treatment of OA.

**Keywords:** Osteoarthritis, osteophytes, stem cells, synovium, periosteum

## INTRODUCTION

A characteristic feature of osteoarthritis (OA) is the formation of osteophytes, which are osteo-cartilaginous outgrowths that typically form at the joint margins, in the region where the synovium attaches to the edge of the articular cartilage and merges with the periosteum. Osteophytes are established through growth of an initial cartilage template that is at least partially replaced with bone containing marrow cavities.[1,2] At later stages, the bone is typically covered by a cartilage cap that can merge with the articular cartilage.[1,2] Despite their high prevalence, the cell populations giving rise to osteophytes in OA remain to be defined.

Several skeletal stem/progenitor cell (SSC) populations have been identified which vary in their ability to form cartilage and bone during skeletal development, maintenance and repair. These include perivascular cells marked by expression of *Pdgfra* and *Sca1*, Nestin (*Nes*), or leptin receptor (*LepR*), and Gremlin-1 (*Grem1*)-expressing cells.[3–9] In addition, during bone regeneration, *Sox9*-expressing progenitors in periosteum initiate cartilage callus formation by giving rise to cells that co-express chondrocyte and osteoblast markers.[10,11] Recently, we used a *Gdf5-Cre* model that is active in the embryonic knee joint interzone, but not in the adult normal or OA knee,[12–14] to show that *Gdf5*-lineage descendants include SSCs in the adult with ability to repair a focal cartilage defect.[15,16] The adult *Gdf5* lineage includes *Prg4*-expressing progenitors in the superficial zone of articular cartilage and synovial lining.[15,17–19]

Here, we show that osteophytes derive from *Pdgfra*-expressing *Gdf5*-lineage cells. These include *Sox9*-expressing progenitors in periosteum that give rise to hybrid skeletal cells that molecularly resemble those observed during bone repair, and *Prg4*-expressing cells from the synovial lining that supply chondrocytes to the outer cartilage layer but do not contribute to bone. Thus, our data define the progenitor cell subsets contributing to osteophyte formation in experimental OA.

## METHODS

### Mice

All animal experimental protocols were approved by the UK Home Office and the Animal Welfare and Ethical Review Committees of the University of Aberdeen and University of Cambridge, the University of Southern California Institutional Animal Care and Use Committee, the Murdoch Children's Research Institute Animal Ethics Committee, or the Animal Use Committee for University Hospital Münster. We used *Col2-CreER*,[20] *Pdgfra-CreER*,[21] *Nes-CreER*,[22] *LepR-Cre*,[23] *Grem1-CreER*,[9] *Gdf5-Cre*,[16] *Prg4-GFP-CreER*,[18] and *Sox9-CreER* mice,[24] Cre-inducible *TdTomato*,[25] *Confetti*,[26] and *mTmG* reporter mice,[27] and *Pdgfra-H2BGFP*[28] and *Nes-GFP*[29] mice (see Supplementary Table 1). Wild-type SWR/J mice were used for *in situ* hybridisation experiments. Mice were maintained on a 12:12 light-dark cycle, in a temperature-controlled room, with water and food *ad libitum*.

### Tamoxifen administration and surgery

Administration of tamoxifen, dissolved in corn oil, was optimised for each mouse strain based on published studies[9,11,18,30,31] and pilot experiments to achieve efficient labelling of intended target cells while minimising impact on animal welfare (see Supplementary Table 2 for details). Adult male mice underwent surgical unilateral destabilisation of the medial meniscus (DMM) through resection of the medial menisco-tibial ligament,[32] with the contralateral knee serving as unoperated or sham-operated control (see Supplementary Table 2 or figure legends for age at surgery). Mice were anaesthetised with ketamine (50 mg/kg) and medetomidine (0.67 mg/kg) with atipamezole (1 mg/kg) post-operatively, ketamine (90 mg/kg) and xylazine (10 mg/kg), or isoflurane with 0.1 mg/kg buprenorphine subcutaneously for analgesia. Proliferating cells were labelled by subcutaneous injection of 2 mg bromodeoxyuridine (BrdU) immediately after surgery followed by 1

mg/ml BrdU in drinking water for 2 weeks. Mice were euthanised for analysis 1, 2 or 8 weeks after surgery. Experimenters were not blinded.

### **Histology and immunohistochemistry**

Tissues were fixed in 4% paraformaldehyde and decalcified in 4-10% EDTA in PBS or 33% (v/v) formic acid with 13.5% (w/v) trisodium citrate dihydrate. Samples were embedded in paraffin or frozen in OCT and sectioned. Sections were stained with safranin-O (Sigma), with or without fast green (Sigma). Fluorescent proteins were either detected by their native fluorescence in cryosections, or via immunofluorescence staining on paraffin sections,[33,34] using antibodies listed in Supplementary Table 3. Sections were counterstained with 4',6-diamidino-2-phenylindole (DAPI; Life technologies), Hoechst, or TO-PRO-3 (ThermoFisher).

### **Imaging**

Images were acquired using a Zeiss Axioscan Z1 slide scanner, Axioskop 40 with Progress XT Core 5 camera, Axio Imager 2.0 and Axio Observer Z1 with AxioCam MRm and AxioCam Mrc, 710 META Laser-Scanning Confocal Microscope, or Nikon AZ100 Microscope with a Nikon Digital sight DS-Fi1 camera. Image analysis was performed using ZEN (Zeiss), ImageJ and QuPath softwares.[35] All analyses were performed on a minimum of 3 sections per sample. Percentages of labelled cells were calculated from the summed cell counts of all sections analysed for each sample, with marrow spaces excluded.

### **RNA *In situ* hybridisation**

Fluorescence RNA *in situ* hybridisation was performed on 7-mm paraffin sections as described.[36] RNA probes[11] were generated following kit instructions (Sigma-Aldrich: 11277073910 and 11685619910) and were detected with Anti-Digoxigenin-POD (Sigma-Aldrich: 11207733910) and

Anti-Fluorescein-POD (Sigma-Aldrich: 11426346910). For double-fluorescence *in situ* hybridisation, the TSA Cyanine 3 and Fluorescein system from Perkin Elmer was used as directed (NEL753001KT).

### **Cell isolation and flow cytometry**

Cells were isolated from mouse knees as described,[15] and stained with fixable viability dye eFluor780 (eBiosciences, Hatfield, UK) and antibodies listed in Supplementary Table 4. Data were acquired on a BD Fortessa flow cytometer and analysed using FlowJo v10 software (Ashland, OR, USA). Unstained and single-labelled cells or antibody-labelled CompBeads (BD Biosciences) were used to set compensation. Debris and doublets were excluded based on Forward and Side Scatter parameters, dead cells were excluded based on viability dye staining, and gates were applied based on Fluorescence-Minus-One controls (Supplementary Fig. 1).

### **Statistical analysis**

Statistical analysis was performed using GraphPad Prism v5. Graphs show data points of individual mice, with mean  $\pm$  95% confidence interval (CI). N-numbers indicate number of mice.

## RESULTS

### **Osteophytes derive from *Pdgfra*-expressing progenitors in periosteum and synovium**

In the DMM model of OA in mice, osteophytes form at the joint margins, often merging with the articular cartilage, similar to human OA.[1,2] We combined the DMM model with genetic cell-labelling and tracing models, to unravel the cell populations giving rise to osteophytes. *Pdgfra* is broadly expressed by mesenchymal stem and progenitor cells. Using *Pdgfra-H2BGFP* mice to identify and trace *Pdgfra*-expressing cells by long-lived GFP expression, we observed GFP+ cells throughout synovium and periosteum of the adult knee (Fig. 1a). In parallel, we tested whether pre-existing articular chondrocytes contribute to osteophyte using *Col2-CreER;ROSA26:loxP-STOP-loxP-TdTomato* (*Tom*) mice treated with tamoxifen at 2 weeks of age, when articular chondrocytes still express high levels of *Col2a1* and are efficiently labelled (Fig. 1b).[30] Two weeks after DMM in tamoxifen-induced *Pdgfra-H2BGFP;Col2-CreER;Tom* mice, GFP+ chondrocytes were present throughout the osteophyte and were negative for Tom (Fig. 1c). Furthermore, there was negligible contribution from Tom+ pre-existing chondrocytes to mature osteophytes at 8 weeks post-DMM (Fig. 1d). These findings indicate that osteophytes do not develop from articular cartilage but derive from *Pdgfra*-expressing stem/progenitor cells.

Next, we induced adult *Pdgfra-CreER;Confetti* mice with tamoxifen to trace individual *Pdgfra*-expressing cells through stochastic expression of membrane-bound CFP, nuclear GFP, cytoplasmic YFP, or cytoplasmic RFP. Negligible fluorescence was detected in the absence of tamoxifen. In unoperated knees of tamoxifen-induced mice, fluorescently labelled cells were observed in periosteum and synovium (Fig. 1e). Consistent with previous studies utilising the *R26-Confetti* reporter,[37,38] GFP was rarely detected and omitted from analysis. Two weeks after DMM, 23.9% (95% CI [17.3%, 30.6%], n=4) of cells in the osteophyte were labelled with either CFP, YFP or RFP (Fig. 1f,g). This may reflect the low sensitivity of the *R26-Confetti* reporter to Cre-mediated

recombination,[17] and aided the identification of distinct clonal cell populations. Intriguingly, clusters of identically coloured chondrocytes, likely derived from individual stem/progenitor cells, were observed in the deep periosteum at the bone surface, while distinct clusters of chondrocyte-like and fibroblast-like cells were found in the overlying synovial tissue (Fig. 1f). These data indicate that *Pdgfra*-expressing stem/progenitor cells clonally expand and give rise to chondrocytes that form osteophytes in experimental OA, and suggest a dual contribution from cells in periosteum and synovium.

### **SSCs marked by expression of *Nes*, *LepR*, or *Grem1* do not give rise to osteophytes**

Since SSC populations marked by expression of *Nes*, *LepR*, or *Grem1* express *Pdgfra*,[3,7–9] we investigated whether they contribute to osteophyte formation. Cells marked by *Nes*-GFP or *Nes*-*CreER*;Tom expression remained confined to vascular niches in synovium, periosteum and bone marrow, likely including pericytes and endothelial cells,[8,9,39] with no detectable contribution to either cartilage or bone of the osteophyte at 2 or 8 weeks post-DMM (Fig. 2a-c). We next analysed *LepR*-*Cre*;Tom mice, since *LepR*-traced cells have been reported to make significant contributions to adult bone turnover and repair following fracture.[8] *LepR*-traced cells were present in synovium and periosteum but negligible contribution to osteophytes was observed (Fig. 2d,e). We also used *Grem1*-*CreER*;Tom mice to trace *Grem1*-expressing SSCs, as they are distinct from *Nes*-GFP+ cells and contribute to fracture repair.[9] Following tamoxifen induction at 7 weeks of age, we found no contribution of *Grem1*-traced cells to osteophytes at 2 weeks post-DMM (Fig. 2f). These data show that *Nes*-, *LepR*-, and *Grem1*-expressing SSCs do not form osteophytes.

### **Osteophytes arise from adult progeny of the *Gdf5*-expressing embryonic joint interzone**

Cells in adult knees that are traced from *Gdf5*-expressing joint interzone cells in the embryo are present in synovium and adjacent periosteum (Fig. 3a), and include SSCs.[15] Analysis of cells



isolated from knees of *Pdgfra-H2BGFP;Gdf5-Cre;Tom* mice (Fig. 3b) revealed that the vast majority of Tom+ *Gdf5*-lineage cells express *Pdgfra*-H2BGFP (93.6%, 95% CI [87.6%, 99.6%], n=9), with *Gdf5*-lineage cells constituting approximately one-third of all *Pdgfra*-H2BGFP+ cells (Fig. 3c,d). Both *Pdgfra*-expressing *Gdf5*-lineage cells (GFP+Tom+) and other *Pdgfra*-expressing cells (GFP+Tom-) expressed, to varying degrees, the mesenchymal stromal cell and fibroblast markers podoplanin (Pdpn/Gp38), CD90, CD73, CD51 and CD105, while neither population included haematopoietic cells (CD45+), endothelial cells (CD31+), or erythrocytes (Ter-119+) (Fig. 3e-h, Supplementary Fig. 1). These findings indicate that adult *Gdf5*-lineage cells are a subset of *Pdgfra*-expressing cells that may form osteophytes.

We thus induced DMM in *Gdf5-Cre;Tom* mice, followed by 2 weeks of BrdU administration to label proliferating cells. At 2 weeks post-DMM, *Gdf5*-lineage cells had extensively proliferated and expanded (Fig. 4a,b), and they were major contributors to Col2-expressing chondrocytes in the osteophytes (Fig. 4b). Tom+ *Gdf5*-lineage cells constituted 82.5% (95% CI [65.1%, 99.8%], n=4), and BrdU+ cells constituted 82.4% (95% CI [69.9%, 94.8%], n=4), of cells within osteophytes at 2 weeks post-DMM (Fig. 4c). Tom+ *Gdf5*-lineage cells remained abundant in mature osteophytes at 8 weeks post-DMM (Fig. 4d). They included 87.7% (95% CI [80.0%, 95.4%], n=7) of cells in the cartilage cap and 70.8% (95% CI [63.6%, 78.1%], n=7) of osteocytes in the bone (Fig. 4e), as well as bone lining cells at endosteal surfaces (Fig. 4d). These data indicate that the *Pdgfra*-expressing progenitors that form osteophytes are largely contained within the joint-resident *Gdf5*-lineage population, which undergo extensive proliferation to supply cells that form both cartilage and bone.

### **Sox9-expressing progenitors give rise to hybrid skeletal cells to initiate osteophytes**

Next, we sought to refine which progenitor populations contribute to osteophytes. Clonal tracing of *Pdgfra*-expressing cells had indicated a possible dual origin from periosteum and synovium (Fig. 1f). Sox9-expressing progenitors in adult periosteum supply skeletal cells to the callus during femoral

fracture repair and large-scale rib regeneration.[10,11] We therefore performed lineage tracing of adult *Sox9*-expressing cells in experimental OA by treating *Sox9-CreER;Tom* mice with tamoxifen prior to DMM surgery. Mice not treated with tamoxifen showed absence of Tom expression. In knees of tamoxifen-treated uninjured mice, Tom<sup>+</sup> cells were detected in periosteum (Fig. 5a). At 2 weeks post-DMM, we observed Tom<sup>+</sup> *Sox9*-traced chondrocytes throughout the early osteophyte (Fig. 5b), thus identifying *Sox9*-expressing progenitors as important contributors of osteophytes.

During regeneration of the adult mouse rib bone, *Sox9*-expressing periosteal cells form a callus composed of hybrid skeletal cells; these “hybrid” cells are characterised by strong co-expression of chondrocyte and osteoblast genes.[11] Similarly, *Col2a1*-expressing cells in the forming osteophyte co-expressed the osteoblast and hypertrophic chondrocyte marker *Ocn* as early as 1 week post-DMM (Fig. 5c). In contrast to growth plate chondrocytes, they also co-expressed *Col1a1* (Fig. 5c), which was particularly apparent in the large osteophytes that typically form on the *Col2-CreER* background (Supplementary Fig. 2). At 2 weeks post-DMM, *Col2a1*-expressing chondrocytes were also positive for the osteoblast and hypertrophic chondrocyte marker *Spp1*, and the hypertrophic chondrocyte marker *Col10a1* (Fig. 5d). We confirmed in the *Sox9-CreER;Tom* model that *Sox9*-traced cells are the source of at least some hybrid cells, based on co-localization of Tom with *Col2a1* and *Col1a1* mRNA expression (Fig. 5e). These findings indicate that the early osteophyte is composed of *Sox9*-derived hybrid skeletal cells similar to those described for rib bone regeneration.

#### **Prg4<sup>+</sup> progenitors contribute to cartilage but not to bone in osteophytes**

The *Gdf5* lineage includes *Prg4*-expressing cells in the synovial lining, which expand in response to acute focal cartilage injury.[17] We therefore investigated whether *Prg4*-expressing cells contribute to osteophyte formation. We first used *Prg4-CreER;ROSA26:loxP-membrane-Tomato-loxP-membrane-GFP (mTmG)* mice induced with tamoxifen at 7 weeks of age. No GFP was detected in mice not treated with tamoxifen. At 2 weeks post-DMM, we observed expansion of GFP<sup>+</sup> *Prg4*-

traced cells in synovium, and *Prg4*-traced cells were found in the outer region of the early osteophyte, while minimal contributions of these cells to the deeper hybrid skeletal cells, expressing *Col2a1* and *Col1a1*, was observed (Fig. 6a,b). To confirm these findings and determine the role of *Prg4*-traced cells at later stages of osteophyte formation, we performed similar *Prg4*-tracing experiments using the Cre-inducible *Tom* reporter model, and extended analysis to 8 weeks post-DMM (Fig. 6c-h). Osteophytes in *Prg4-CreER;Tom* mice at 2 weeks post-DMM were typically more advanced than those observed in the *Prg4-CreER;mTmG* model, with a layer of cartilage surrounding a hypertrophic centre undergoing remodelling to bone (Fig. 6d). As well as expanding in synovium, Tom+ *Prg4*-traced cells constituted 41.9% (95% CI [27.7%, 56.1%], n=8) of chondrocytes embedded in a cartilage matrix immunostaining for Col2 (Fig. 6d,e). Consistent with the data in the *Prg4-CreER;mTmG* model (Fig. 6b), they were predominantly found in the outer region, with some contribution to Col10-expressing hypertrophic chondrocytes in deeper regions of the osteophyte (Fig. 6f). At 8 weeks post-DMM, Tom+ *Prg4*-traced cells persisted in the cartilage cap covering the mature osteophyte but were barely detected in bone (Fig. 6g,h). Thus, *Prg4*-lineage cells from the overlying synovial tissue supply chondrocytes to the forming osteophyte, and while they persist in the cartilage cap of the mature osteophyte, they make negligible contributions to bone.

## DISCUSSION

Osteophytes are a key feature of OA, and their occurrence is a criterion for imaging-based diagnosis of OA.[40] In peripheral joint OA, osteophytes are associated with pain, knee structural progression and incidence of joint replacement.[41-43] Nonetheless, research in OA pathogenesis has largely focused on mechanisms of articular cartilage breakdown, while the extensive joint remodelling events have been considered secondary. Osteophytes, however, are not always linked to severity of articular cartilage loss.[44] Understanding the biology of osteophyte formation will provide critical insights in the mechanisms underlying the structural derangements that occur in OA joints.

We show that osteophytes primarily arise from descendants of *Gdf5*-expressing embryonic joint interzone cells that reside in the adult knee. Together with our previous data showing that *Gdf5*-lineage cells underpin synovial hyperplasia and cartilage repair after injury,[15] these findings point to a central role of *Gdf5*-lineage cells in the maintenance, repair, and remodelling of adult joint tissues. Although osteophytes typically develop close to articular cartilage, *Col2a1*-expressing chondrocytes from articular cartilage did not give rise to osteophytes. Instead, we show that osteophytes originate at least in part from a population of *Sox9*-expressing progenitors in periosteum, with progeny of *Prg4*-expressing synovial-lining cells supplying chondrocytes to the cartilage but not osteoblast-lineage cells that form the bone of the osteophyte.

Several SSC populations have been implicated in bone fracture repair, including SSCs identified by expression of *Nes*, *LepR*, or *Grem1*. [4,8,9,45] We observed negligible contribution of these SSC populations to osteophytes in OA. Yet intriguingly, our data indicate that the initial stages of osteophyte formation are similar to endochondral bone repair in the mouse femur,[10] rib,[11] and zebrafish lower jaw.[36] During bone repair, *Sox9*-expressing cells in periosteum supply chondrocytes and osteoblasts, and help to orchestrate callus formation.[10,11] Furthermore, the

early callus of the regenerating rib includes *Sox9*-lineage cells with a hybrid chondrocyte/osteoblast identity,[11] similar to what we observed in the early stages of osteophyte formation.

Until this study, it was not known whether the osteophyte derives from a single progenitor population, or whether multiple progenitor populations cooperate to form the different tissue layers of the osteophyte. Our data indicate that within the *Gdf5*-lineage population that forms all parts of the osteophyte, periosteal *Sox9*-expressing progenitors give rise to the deeper hybrid cells that form the ossifying cartilage template, while synovial *Prg4*-expressing cells supply chondrocytes but make negligible contributions to osteoblast-lineage cells. Recently, it was shown that joint development occurs through a continuous influx of new cells into the *Gdf5*-expressing joint interzone and flanking regions, with cells being temporally specified to contribute differentially to the multiple tissues of the joint.[17,46] Our data show that lineage fate determination persists in the adult joint between sub-populations of *Gdf5*-lineage cells and suggest the co-existence of distinct progenitor cell subsets with restricted differentiation potential that may have become imprinted through development.

Human osteophytes in OA hip and knee joints share similar pathological features to those seen in mice, with endochondral bone covered by a cartilage cap that merges with or overgrows the articular cartilage.[2] Notably, our molecular phenotype data in mouse is consistent with observations in human, where an overlap of *Col1* and *Col2* expression is found in the early stages of osteophyte formation, and chondrocytes in the osteophyte express osteocalcin.[2,47] Adult human synovium and periosteum are known to contain mesenchymal progenitors,[48,49] which may retain the ability to orchestrate an aberrant joint morphogenetic process.[15] Various molecular factors and pathways have been implicated in osteophyte formation, including  $TGF\beta$  and BMP signalling[1]. Here, we propose a model whereby joint-resident progenitor cell subsets in periosteum and synovium that ontogenetically derive from the embryonic joint interzone respond to such signals and cooperate to form osteophytes in OA (Figure 7). Our data define progenitor cell subsets that could be targeted as part of disease modification strategies for treatment of OA.

## **ACKNOWLEDGEMENTS**

The authors thank all members of the Arthritis & Regenerative Medicine Laboratory at the University of Aberdeen; Shina Ardani and William Alton for their contributions to data acquisition; Animal Facility staff for care of our animals; staff in the Microscopy and Histology Facility and Iain Fraser Cytometry Centre at the University of Aberdeen.

## **FUNDING**

C.D.B., A.J.Ro, K.K., A.J.Ra., F.C. and H.W. were supported by funding from Versus Arthritis, formerly Arthritis Research UK (20775, 21156, 20050, 19429), and the Medical Research Council (MR/L020211/1). T.P., J.Sh., M.Sa., and R.G. were supported by funding from the Bundesministerium für Bildung und Forschung (BMBF) Overload-PrevOP consortium (01EC1408F) and the Innovative Medizinische Forschung (IMF) Program of the University Hospital Münster (Project I-SH121608). J.G.C., S.T.K. J.Sm., M.A.S., and F.V.M. were supported by funding from R01 AR069700. J.F.B, L.R. and C.B.L were supported by the National Health and Medical Research Council (NHMRC: APP1063133), and part funding was provided to J.F.B. by the Victorian Government's Operational Infrastructure Support Program to the Murdoch Children's Research Institute. C.K. and S.M.F. were supported by funding from the Wellcome Trust (203151/Z/16/Z), Horizon2020 (ERC-2014-CoG-648765), Cancer Research UK (C61367/A26670) and NHS Blood and Transplant.

## **AUTHOR CONTRIBUTIONS**

A.J.Ro.: Conceptualisation, experimental design, data acquisition, analysis and interpretation, writing of the manuscript; K.K.: Experimental design, data acquisition, analysis and interpretation, contributed to writing of the manuscript; A.J.Ra., F.C.: Data acquisition, analysis and interpretation, contributed to writing of the manuscript. M.Sa., S.K.: Data acquisition, analysis and interpretation;

J.Sm., M.Se., L.R., C.B.L.: Data acquisition and analysis; H.W., R.G.: Data acquisition; C.K., S.M.F.: Experimental design and data acquisition; F.V.M., T.P., J.F.B.: Conceptualisation, experimental design, data interpretation; J.Sh.: Conceptualisation, experimental design, data acquisition, analysis and interpretation; J.G.C.: Conceptualisation, experimental design, data acquisition, analysis and interpretation, contributed to writing of the manuscript; C.D.B.: Conceptualisation, experimental design, data analysis and interpretation, writing of the manuscript.

#### **COMPETING INTERESTS**

The authors declare no competing financial interests.

#### **DATA AVAILABILITY**

All data supporting the findings of this study are available within the Article and its Supplementary Information files, or are available from the corresponding authors upon reasonable request.

## REFERENCES

- 1 Van der Kraan PM, Van den Berg WB. Osteophytes: relevance and biology. *Osteoarthr Cartil* 2007;15:237–44. doi:10.1016/j.joca.2006.11.006
- 2 Gelse K, Söder S, Eger W, *et al.* Osteophyte development—molecular characterization of differentiation stages. *Osteoarthr Cartil* 2003;11:141–8. doi:10.1053/joca.2002.0873
- 3 Morikawa S, Mabuchi Y, Kubota Y, *et al.* Prospective identification, isolation, and systemic transplantation of multipotent mesenchymal stem cells in murine bone marrow. *J Exp Med* 2009;206:2483–96.
- 4 Mendez-Ferrer S, Michurina T V, Ferraro F, *et al.* Mesenchymal and haematopoietic stem cells form a unique bone marrow niche. *Nature* 2010;466:829–34.
- 5 Yamazaki S, Ema H, Karlsson G, *et al.* Nonmyelinating Schwann cells maintain hematopoietic stem cell hibernation in the bone marrow niche. *Cell* 2011;147:1146–58. doi:10.1016/j.cell.2011.09.053
- 6 Kunisaki Y, Bruns I, Scheiermann C, *et al.* Arteriolar niches maintain haematopoietic stem cell quiescence. *Nature* 2013;502:637–43. doi:10.1038/nature12612
- 7 Pinho S, Lacombe J, Hanoun M, *et al.* PDGFR $\alpha$  and CD51 mark human Nestin+ sphere-forming mesenchymal stem cells capable of hematopoietic progenitor cell expansion. *J Exp Med* 2013;210:1351–67. doi:10.1084/jem.20122252
- 8 Zhou BO, Yue R, Murphy MM, *et al.* Leptin-receptor-expressing mesenchymal stromal cells represent the main source of bone formed by adult bone marrow. *Cell Stem Cell* 2014;15:154–68. doi:10.1016/j.stem.2014.06.008
- 9 Worthley DL, Churchill M, Compton JT, *et al.* Gremlin 1 Identifies a Skeletal Stem Cell with Bone, Cartilage, and Reticular Stromal Potential. *Cell* 2015;160:269–84.



doi:10.1016/j.cell.2014.11.042

- 10 He X, Bougioukli S, Ortega B, *et al.* Sox9 positive periosteal cells in fracture repair of the adult mammalian long bone. *Bone* 2017;103:12–9. doi:10.1016/j.bone.2017.06.008
- 11 Kuwahara ST, Serowoky MA, Vakhshori V, *et al.* Sox9+ messenger cells orchestrate large-scale skeletal regeneration in the mammalian rib. *Elife* 2019;8. doi:10.7554/eLife.40715
- 12 Chen H, Capellini TD, Schoor M, *et al.* Heads, Shoulders, Elbows, Knees, and Toes: Modular Gdf5 Enhancers Control Different Joints in the Vertebrate Skeleton. *PLoS Genet* 2016;12:e1006454. doi:10.1371/journal.pgen.1006454
- 13 Pregizer SK, Kiapour AM, Young M, *et al.* Impact of broad regulatory regions on *Gdf5* expression and function in knee development and susceptibility to osteoarthritis. *Ann Rheum Dis* 2018;;annrheumdis-2017-212475. doi:10.1136/annrheumdis-2017-212475
- 14 Kania K, Colella F, Riemen AHK, *et al.* Regulation of Gdf5 expression in joint remodelling, repair and osteoarthritis. *Sci Rep* 2020;10:157. doi:10.1038/s41598-019-57011-8
- 15 Roelofs AJ, Zupan J, Riemen AHK, *et al.* Joint morphogenetic cells in the adult mammalian synovium. *Nat Commun* 2017;8:15040. doi:10.1038/ncomms15040
- 16 Rountree RB, Schoor M, Chen H, *et al.* BMP Receptor Signaling Is Required for Postnatal Maintenance of Articular Cartilage. *PLoS Biol* 2004;2:e355. doi:10.1371/journal.pbio.0020355
- 17 Decker RS, Um H-B, Dymont NA, *et al.* Cell origin, volume and arrangement are drivers of articular cartilage formation, morphogenesis and response to injury in mouse limbs. *Dev Biol* 2017;426:56–68. doi:10.1016/j.ydbio.2017.04.006
- 18 Kozhemyakina E, Zhang M, Ionescu A, *et al.* Identification of a Prg4-expressing articular cartilage progenitor cell population in mice. *Arthritis Rheumatol (Hoboken, NJ)* 2015;67:1261–73. doi:10.1002/art.39030

- 19 Li L, Newton PT, Boudierlique T, *et al.* Superficial cells are self-renewing chondrocyte progenitors, which form the articular cartilage in juvenile mice. *FASEB J* 2017;31:1067–84. doi:10.1096/fj.201600918R
- 20 Nakamura E, Nguyen M-T, Mackem S. Kinetics of tamoxifen-regulated Cre activity in mice using a cartilage-specific CreER(T) to assay temporal activity windows along the proximodistal limb skeleton. *Dev Dyn* 2006;235:2603–12. doi:10.1002/dvdy.20892
- 21 Kang SH, Fukaya M, Yang JK, *et al.* NG2+ CNS glial progenitors remain committed to the oligodendrocyte lineage in postnatal life and following neurodegeneration. *Neuron* 2010;68:668–81. doi:10.1016/j.neuron.2010.09.009
- 22 Balordi F, Fishell G. Mosaic Removal of Hedgehog Signaling in the Adult SVZ Reveals That the Residual Wild-Type Stem Cells Have a Limited Capacity for Self-Renewal. *J Neurosci* 2007;27:14248–59. doi:10.1523/JNEUROSCI.4531-07.2007
- 23 Leshan RL, Björnholm M, Münzberg H, *et al.* Leptin Receptor Signaling and Action in the Central Nervous System. *Obesity* 2006;14:208S–212S. doi:10.1038/oby.2006.310
- 24 Soeda T, Deng JM, de Crombrughe B, *et al.* Sox9-expressing precursors are the cellular origin of the cruciate ligament of the knee joint and the limb tendons. *Genesis* 2010;48:635–44. doi:10.1002/dvg.20667
- 25 Madisen L, Zwingman TA, Sunkin SM, *et al.* A robust and high-throughput Cre reporting and characterization system for the whole mouse brain. *Nat Neurosci* 2010;13:133–40.
- 26 Snippert HJ, van der Flier LG, Sato T, *et al.* Intestinal Crypt Homeostasis Results from Neutral Competition between Symmetrically Dividing Lgr5 Stem Cells. *Cell* 2010;143:134–44. doi:10.1016/j.cell.2010.09.016
- 27 Muzumdar MD, Tasic B, Miyamichi K, *et al.* A global double-fluorescent Cre reporter mouse. *Genesis* 2007;45:593–605.

- 28 Hamilton TG, Klinghoffer RA, Corrin PD, *et al.* Evolutionary divergence of platelet-derived growth factor alpha receptor signaling mechanisms. *Mol Cell Biol* 2003;23:4013–25. doi:10.1128/mcb.23.11.4013-4025.2003
- 29 Mignone JL, Kukekov V, Chiang AS, *et al.* Neural stem and progenitor cells in nestin-GFP transgenic mice. *J Comp Neurol* 2004;469:311–24.
- 30 Nagao M, Cheong CW, Olsen BR. Col2-Cre and tamoxifen-inducible Col2-CreER target different cell populations in the knee joint. *Osteoarthr Cartil* 2016;24:188–91. doi:10.1016/j.joca.2015.07.025
- 31 Isern J, García-García A, Martín AM, *et al.* The neural crest is a source of mesenchymal stem cells with specialized hematopoietic stem cell niche function. *Elife* 2014;3:e03696. doi:10.7554/eLife.03696
- 32 Glasson SS, Blanchet TJ, Morris EA. The surgical destabilization of the medial meniscus (DMM) model of osteoarthritis in the 129/SvEv mouse. *Osteoarthritis Cartilage* 2007;15:1061–9. doi:10.1016/j.joca.2007.03.006
- 33 Kurth TB, Dell’Accio F, Crouch V, *et al.* Functional mesenchymal stem cell niches in adult mouse knee joint synovium in vivo. *Arthritis Rheum* 2011;63:1289–300.
- 34 Roelofs AJ, De Bari C. Immunostaining of Skeletal Tissues. In: *Methods in molecular biology (Clifton, N.J.)*. Humana Press 2019. 437–50. doi:10.1007/978-1-4939-8997-3\_25
- 35 Bankhead P, Loughrey MB, Fernández JA, *et al.* QuPath: Open source software for digital pathology image analysis. *Sci Rep* 2017;7:16878. doi:10.1038/s41598-017-17204-5
- 36 Paul S, Schindler S, Giovannone D, *et al.* Ihha induces hybrid cartilage-bone cells during zebrafish jawbone regeneration. *Development* 2016;143:2066–76. doi:10.1242/dev.131292
- 37 Snippert HJ, van der Flier LG, Sato T, *et al.* Intestinal crypt homeostasis results from neutral

- competition between symmetrically dividing Lgr5 stem cells. *Cell* 2010;143:134–44.
- 38 Baggiolini A, Varum S, Mateos JM, *et al.* Premigratory and Migratory Neural Crest Cells Are Multipotent In Vivo. *Cell Stem Cell* 2015;16:314–22. doi:10.1016/j.stem.2015.02.017
- 39 Ono N, Ono W, Mizoguchi T, *et al.* Vasculature-associated cells expressing nestin in developing bones encompass early cells in the osteoblast and endothelial lineage. *Dev Cell* 2014;29:330–9. doi:10.1016/j.devcel.2014.03.014
- 40 Altman R, Asch E, Bloch D, *et al.* Development of criteria for the classification and reporting of osteoarthritis. Classification of osteoarthritis of the knee. Diagnostic and Therapeutic Criteria Committee of the American Rheumatism Association. *Arthritis Rheum* 1986;29:1039–49. doi:10.1002/art.1780290816
- 41 Barr AJ, Campbell TM, Hopkinson D, *et al.* A systematic review of the relationship between subchondral bone features, pain and structural pathology in peripheral joint osteoarthritis. *Arthritis Res Ther* 2015;17:228. doi:10.1186/s13075-015-0735-x
- 42 Hunter D, Nevitt M, Lynch J, *et al.* Longitudinal validation of periarticular bone area and 3D shape as biomarkers for knee OA progression? Data from the FNIH OA Biomarkers Consortium. *Ann Rheum Dis* 2016;75:1607-14. doi: 10.1136/annrheumdis-2015-207602
- 43 Bowes MA, Maciewicz RA, Waterton JC, *et al.* Bone area provides a responsive outcome measure for bone changes in short-term knee osteoarthritis studies. *J Rheumatol* 2016;43:2179-82. doi: 10.3899/jrheum.151118
- 44 Waldstein W, Kasperek MF, Faschingbauer M, *et al.* Lateral-compartment Osteophytes are not Associated With Lateral-compartment Cartilage Degeneration in Arthritic Varus Knees. *Clin Orthop Relat Res* 2017;475:1386–92. doi:10.1007/s11999-016-5155-y
- 45 Tournaire G, Stegen S, Giacomini G, *et al.* Nestin-GFP transgene labels skeletal progenitors in the periosteum. *Bone* 2020;133:115259. doi:10.1016/j.bone.2020.115259

- 46 Shwartz Y, Viukov S, Krief S, *et al.* Joint Development Involves a Continuous Influx of Gdf5-Positive Cells. *Cell Rep* 2016;15:2577–87. doi:10.1016/j.celrep.2016.05.055
- 47 Gelse K, Ekici AB, Cipa F, *et al.* Molecular differentiation between osteophytic and articular cartilage – clues for a transient and permanent chondrocyte phenotype. *Osteoarthr Cartil* 2012;20:162–71. doi:10.1016/j.joca.2011.12.004
- 48 De Bari C, Dell’Accio F, Tylzanowski P, *et al.* Multipotent mesenchymal stem cells from adult human synovial membrane. *Arthritis Rheum* 2001;44:1928–42.
- 49 De Bari C, Dell’Accio F, Luyten FP. Human periosteum-derived cells maintain phenotypic stability and chondrogenic potential throughout expansion regardless of donor age. *Arthritis Rheum* 2001;44:85–95.

## FIGURE LEGENDS

**Figure 1. *Pdgfra*-lineage progenitors, not articular chondrocytes, clonally expand to form osteophytes.**

(a) GFP expression (green) by cells in periosteum and synovium of the knee of a 15-week-old mouse carrying the *Pdgfra-H2BGFP* transgene (n=2). (b) Eight-week-old *Col2-CreER;Tom* mice induced with tamoxifen at 2 weeks of age (n=8, 2 experiments, 7-8 weeks old). Note Tom-labelled cells (red) in articular and growth plate cartilage of the knee. (c) *Pdgfra-H2BGFP;Col2-CreER; Tom* mice induced with tamoxifen at 2 weeks of age and analysed 2 weeks after DMM (n=4, plus n=3 *Col2-CreER;Tom* only). Note *Pdgfra*-expressing cells (green) in osteophyte that are negative for Tom (red). (d) Tom expression (red) in *Col2-CreER;Tom* mice induced with tamoxifen at 2 weeks of age and analysed 8 weeks after DMM (n=6). (e-g) *Pdgfra-CreER;Confetti* mice were induced with tamoxifen from 11-12 weeks of age, followed by DMM surgery and analysis 2 weeks later (n=4). (e) CFP (blue), YFP (yellow) and RFP (red) expression in contralateral knee serving as internal control. Arrows indicate labelled cells along periosteal surface. (f) CFP (blue), YFP (yellow) and RFP (red) expression in osteophyte of destabilised knee. Arrows indicate monochromatic chondrocyte clusters within periosteum, arrowheads indicate distinct monochromatic clusters of chondrocyte-like and fibroblast-like cells in overlying synovium. (g) Percentage of cells in osteophytes labelled with each of the fluorescent proteins, and total percentage of cells labelled (mean  $\pm$  95% CI, n=4). Fluorescence microscopy images in (a,b,d) show nuclear counterstain in blue. Dashed white lines in (c,d,f) indicate boundary between osteophyte and edge of tibia. Brightfield images of near-adjacent sections stained with Safranin O and Fast Green are shown on the left in (c-f). A: Articular cartilage, G: Growth plate, PS: Periosteum and Synovium junction, S: Synovium. Scale bars in all panels indicate 100  $\mu$ m.

**Figure 2. Perivascular and *Grem1*-expressing skeletal stem cells do not contribute to osteophyte formation.**

(a-c) *Nes-CreER;Tom* mice, some also carrying *Nes-GFP*, were induced with tamoxifen neonatally. (a) *Nes*-traced cells (red) and *Nes-GFP*<sup>+</sup> cells (green) in knee from 13-week-old unoperated mouse (n=3, 2 experiments, 6-13 weeks old). (b) *Nes*-traced cells (red, n=6) and *Nes-GFP*<sup>+</sup> cells (green, n=3) in knee 2 weeks post-DMM. Arrows indicate labelled cells around blood vessels in synovium. (c) *Nes*-traced cells (red) in knee 8 weeks post-DMM (n=3). Arrows indicate labelled cells associated with bone marrow vasculature within osteophyte. (d,e) *LepR-Cre;Tom* mice underwent DMM surgery at 12 weeks and were analysed 8 weeks later. (d) *LepR*-traced cells (red) in uninjured contralateral knee serving as internal control (n=3). Arrows indicate labelled cells in synovium and periosteum. (e) *LepR*-traced cells (red) in destabilised knee (n=4). Arrows indicate labelled cells in synovium. (f) *Grem1-CreER;Tom* mice were induced with tamoxifen at 7 weeks of age and left unoperated (n=2) or analysed 2 weeks after DMM (n=3). Arrow indicates osteophyte. Fluorescence microscopy images in all panels show nuclear counterstain in blue. Dashed white lines in (b,c,e) indicate boundary between osteophyte and edge of tibia. Brightfield images of near-adjacent sections stained with Safranin O and Fast Green are shown on the left in (a-e). A: Articular cartilage, G: Growth plate, PS: Periosteum and Synovium junction, S: Synovium. Scale bars in all panels indicate 100  $\mu$ m.

**Figure 3. *Gdf5*-lineage cells are a subset of *Pdgfra*-expressing cells in the adult knee.**

(a) Tom<sup>+</sup> *Gdf5*-lineage cells (red) in 14-week-old *Gdf5-Cre;Tom* mouse knee. Nuclear counterstain is shown in blue. A: Articular cartilage, PS: Periosteum and Synovium junction, S: Synovium. Scale bar indicates 100  $\mu$ m. (b) Knee of 11-week-old *Pdgfra-H2BGFP;Gdf5-Cre;Tom* mouse showing Tom (red; *Gdf5*-lineage cells) and GFP expression (green; *Pdgfra*-expressing cells) (n=3). A: Articular cartilage, G: Growth plate, PS: Periosteum and Synovium junction, S: Synovium. Scale bar indicates 100  $\mu$ m. (c-h) Freshly isolated cells from knees of *Pdgfra-H2BGFP;Gdf5-Cre;Tom* mice (7-10 weeks old) were

analysed by flow cytometry. See Supplementary Fig. 1 for gating strategies and FMO controls. (c) Representative flow plot showing Tom and GFP expression by single viable cells (n=9, 4 experiments). (d) Percentage of single viable cells that expressed one or both fluorescent labels (mean  $\pm$  95% CI, n=9, 4 experiments). (e-h) Phenotypic analysis detecting a range of mesenchymal and fibroblast (Gp38, CD90, CD73, CD51, and CD105), haematopoietic (CD45), endothelial (CD31), or erythrocyte (Ter-119) markers. (e) Representative flow plots showing expression of Tom and the indicated markers within single viable GFP+ cells (n=4-5 for each marker, 4 experiments). (f-h) Percentage of single viable cells that express the indicated markers within (f) GFP+Tom+ (*Gdf5*-lineage cells), (g) GFP+Tom- (other *Pdgfra*-expressing cells), and (h) GFP-Tom- cell populations (mean  $\pm$  95% CI, n=4-5 for each marker, 4 experiments).

**Figure 4. Joint-resident SSCs within the *Gdf5*-lineage form osteophytes.**

(a-c) Adult *Gdf5-Cre;Tom* mice underwent surgery at 9 weeks to induce DMM in one knee, with contralateral knee sham-operated, and BrdU administered from surgery until end of experiment 2 weeks later. (a) Tom+ *Gdf5*-lineage cells (red) and BrdU-labelled cells (green) in sham-operated knee (n=4). Arrows indicate Tom+ cells along the periosteal surface with incorporated proliferation label. (b) Tom+ *Gdf5*-lineage cells (red) and BrdU-labelled cells (green) in destabilised knee (n=4). Note Tom+ cells with incorporated proliferation label throughout the osteophyte. Co-staining for Tom (red) with Col2 (green) to reveal cartilage matrix surrounding Tom+ cells is shown on the far right (image from different mouse). (c) Percentage of cells in osteophytes that are Tom+ *Gdf5*-lineage cells, and percentage of cells in osteophytes that have incorporated the BrdU proliferation label (mean  $\pm$  95% CI, n=4). (d,e) *Gdf5-Cre;Tom* mice underwent DMM surgery at 9-14 weeks and were analysed 8 weeks after DMM. (d) Tom+ *Gdf5*-lineage cells (red) in mature osteophyte (n=7). Arrows indicate Tom+ bone lining cells along endosteal surfaces and arrowheads indicate Tom+ osteocytes embedded within bone of the osteophyte. Enlarged image on right shows Tom+ chondrocytes in the



cartilage cap. **(e)** Percentage of cells in osteophytes that are Tom+ *Gdf5*-lineage cells (mean  $\pm$  95% CI, n=7), divided into the cartilage cap region, and osteocytes within bone. Fluorescence microscopy images in all panels show nuclear counterstain in blue. Dashed white lines in **(b,d)** indicate boundary between osteophyte and edge of tibia. Brightfield images of near-adjacent sections stained with Safranin O and Fast Green are shown on the left. Boxed regions indicate areas shown at higher magnification on the right. A: Articular cartilage, G: Growth plate, PS: Periosteum and Synovium junction, S: Synovium. Scale bars in all panels indicate 100  $\mu$ m.

**Figure 5. Sox9-expressing progenitors give rise to hybrid cells in the early osteophyte.**

**(a,b,e)** *Sox9-CreER;Tom* mice were induced with tamoxifen at 7 weeks of age. **(a)** Tom+ *Sox9*-traced cells (red) in articular cartilage (A), growth plate (G), and scattered within periosteum (P) of knee from 9-week-old uninjured mouse (n=3). Boxed region on left indicates area shown at higher magnification on the right (different tissue sections are shown). **(b)** Tom+ *Sox9*-traced cells (red) throughout osteophyte (outlined with dashed white line on far right) at 2 weeks post-DMM (n=3). Brightfield image of near-adjacent section stained with Safranin O and Fast Green is shown on the left. Boxed region is shown at higher magnification on the far right. A: Articular cartilage, G: growth plate. **(c,d)** Double fluorescence *in situ* hybridisation in wild-type mouse knees at 1 week **(c)** or 2 weeks post-DMM **(d)** for indicated mRNA targets. Note co-expression of *Col2a1* (red) with *Col1a1*, *Ocn*, *Spp1*, or *Col10a1* (green) in the early osteophyte, and absence of *Col1a1* in the tibial growth plate (G). Merged and individual channel images of the boxed osteophytes are shown to the right. n=3 for each probe combination. **(e)** Co-detection of Tom with *Col2a1* and *Col1a1* mRNA in osteophyte of *Sox9-CreER;Tom* mouse (n=3). Individual and merged channel images are shown. Note Tom+ *Sox9*-traced cells (magenta) co-expressing *Col2a1* (green) and *Col1a1* (red) in outlined area. Fluorescence microscopy images in all panels show nuclear counterstain in blue. Scale bars indicate 100  $\mu$ m in **(a,b)** and 200  $\mu$ m in **(c-e)**.

**Figure 6. Contribution of *Prg4*-expressing progenitors to osteophytes.**

(a,b) *Prg4-CreER;mTmG* mice were induced with tamoxifen at 7 weeks of age, followed by surgery to induce DMM in one knee, with contralateral knee sham-operated. *Prg4*-traced cells were detected with anti-GFP antibody (green), and *Col1a1* or *Col2a1* mRNA expression by fluorescence *in situ* hybridisation (red). (a) GFP+ *Prg4*-traced cells at articular surface and in synovial lining in control sham-operated knee (n=3). Note membrane localisation of GFP, indicating successful *mTmG* conversion. (b) GFP+ *Prg4*-traced cells at 2 weeks post-DMM. Note expansion in synovium but minimal contribution to hybrid cells that express *Col1a1* and *Col2a1* in the early osteophyte (n=3). Boxes indicate magnified images to the right, shown as merged and individual channels. Arrowheads indicate rare *Prg4*-traced cells expressing *Col2a1*. (c-h) *Prg4-CreER;Tom* mice were induced with tamoxifen at 8 weeks of age. (c) Tom+ *Prg4*-traced cells (red) in synovial lining and superficial zone of articular cartilage in 10-week-old uninjured mouse (n=7, 3 experiments). Green: Col2 immunostaining (n=3). (d) Tom+ *Prg4*-traced cells (red) in osteophyte at 2 weeks post-DMM (n=8, 2 experiments). Note Tom+ cells in Col2+ (green) cartilage matrix and overlying synovial tissue. (e) Percentage of cells that expressed Tom at 2 weeks post-DMM in Col2+ cartilage matrix or Col2- tissue of the osteophyte (mean  $\pm$  95% CI, n=8, 2 experiments). (f) Tom+ *Prg4*-traced cells (red) in Col10+ (green) hypertrophic cartilage of osteophyte 2 weeks post-DMM, indicated by arrows (n=4). (g) Tom+ *Prg4*-traced cells (red) in osteophyte at 8 weeks post-DMM (n=7, 2 experiments). Green: Col2 immunostaining. (h) Percentage of cells that expressed Tom at 8 weeks post-DMM in Col2+ cartilage matrix or Col2- tissue of the osteophyte cap, or among osteocytes in the osteophyte bone (mean  $\pm$  95% CI, n=7, 2 experiments). Fluorescence microscopy images show nuclear counterstain in blue. Brightfield images of Safranin-O-stained near-adjacent sections are shown on the left in (d,g). Dashed white lines indicate boundary between osteophyte and edge of tibia in (d,f,g). A: Articular cartilage, G: Growth plate, PS: Periosteum and Synovium junction, S: Synovium. Scale bars indicate 200  $\mu$ m in (a,b) and 100  $\mu$ m in (c,d,f,g).

### **Figure 7. Proposed model of osteophyte formation in OA.**

Our data show that *Pdgfra*<sup>+</sup> *Gdf5*-lineage progenitors, which in the normal joint are present at the junction of periosteum and synovium near the articular cartilage, are activated in OA to form both the cartilage and bone of the osteophyte. They include *Prg4*-expressing progenitors (orange) residing in synovial lining and *Sox9*-expressing progenitors (green) in the underlying periosteum. During the early stage of osteophyte formation, *Sox9*-expressing progenitors in periosteum give rise to hybrid skeletal cells that form a transient cartilage template which is remodelled to bone. Progeny of *Prg4*-expressing progenitors are recruited to the forming osteophyte and supply chondrocytes to the cartilage, but they make negligible contributions to osteoblast-lineage cells that form the bone. A: Articular cartilage, M: meniscus.

### **KEY MESSAGES**

#### **What is already known about this subject?**

Osteophytes are a key feature of osteoarthritis. Several skeletal stem and progenitor cell populations have been identified; however, their contribution to osteophyte formation remains unexplored.

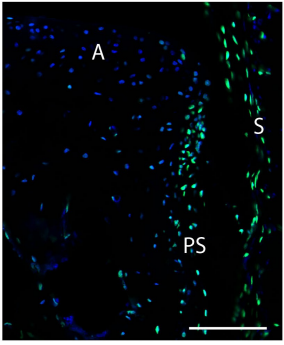
#### **What does this study add?**

This study shows that descendants of the *Gdf5*-expressing cells of the embryonic joint interzone form osteophytes in osteoarthritis, and reveals contributions of two distinct progenitor cell populations residing in periosteum and synovium.

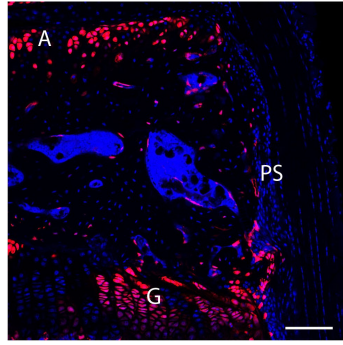
#### **How might this impact on clinical practice or future developments?**

This study defines the progenitor cell subsets forming the osteophytes, which could be targeted as part of disease modification strategies for treatment of osteoarthritis.

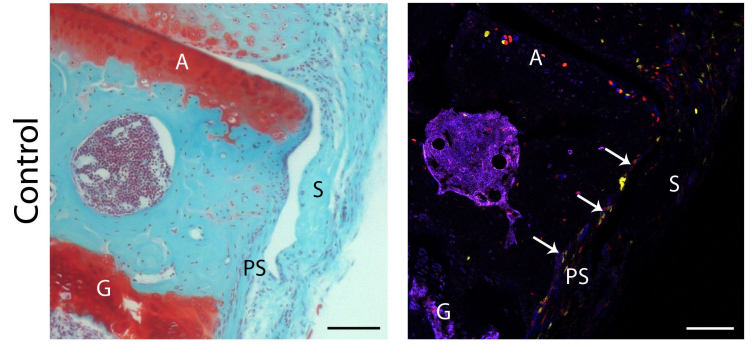
**a** *Pdgfra-H2B***GFP**



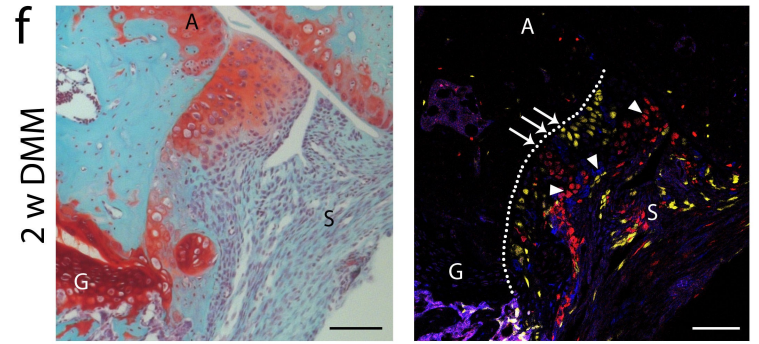
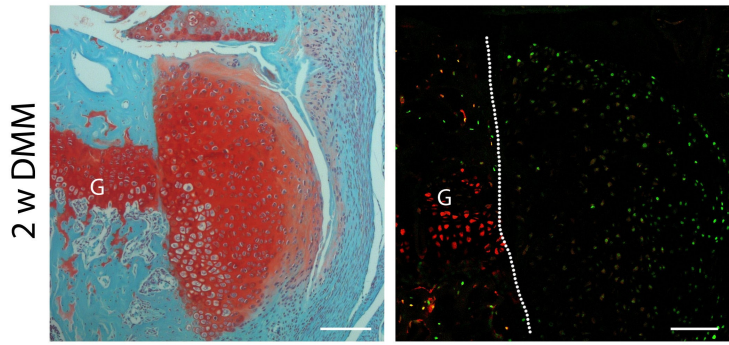
**b** *Col2-CreER; Tom*, induction at 2 w



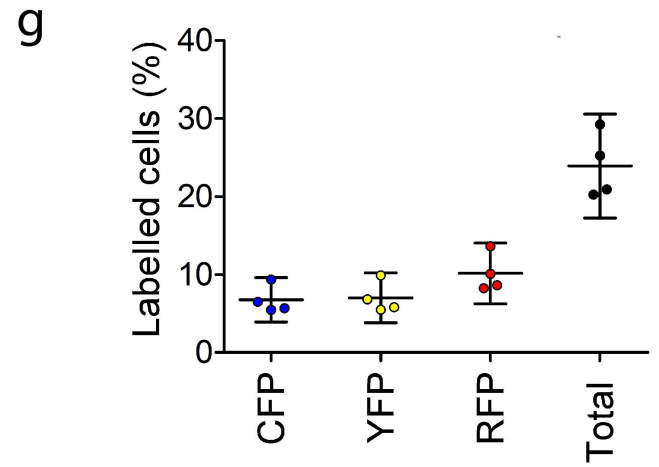
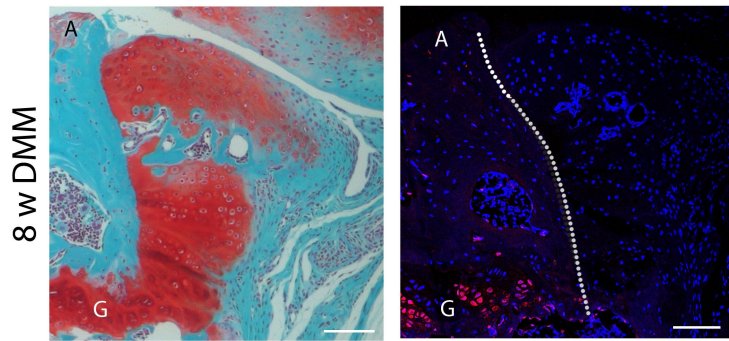
**e** *Pdgfra-CreER; Confetti*, induction from 11 w



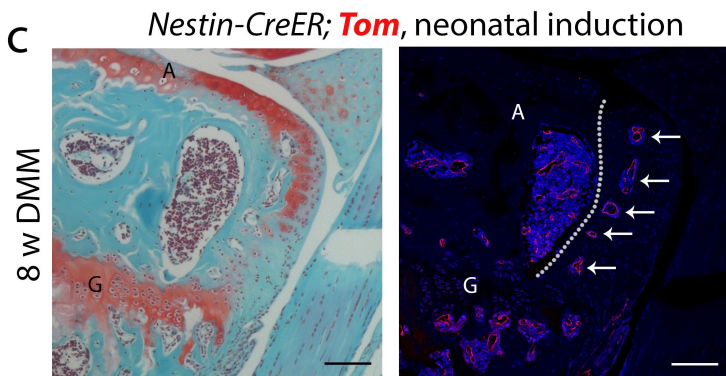
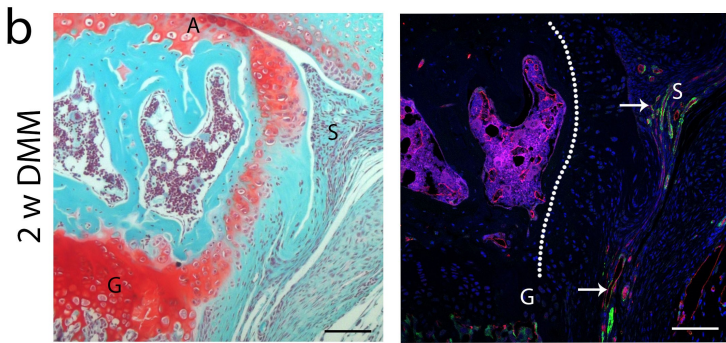
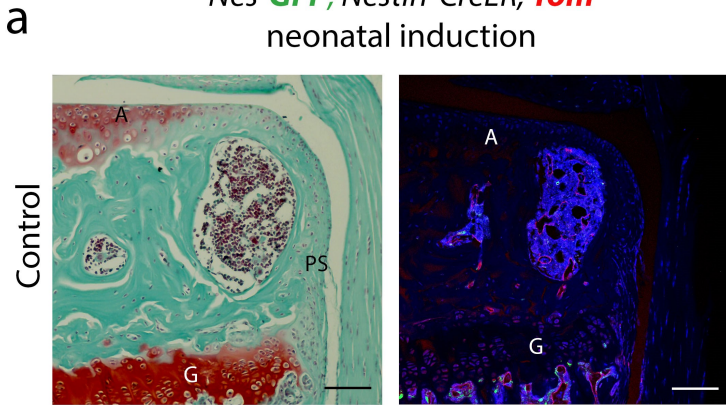
**c** *Pdgfra-H2B***GFP**; *Col2-CreER; Tom*, induction at 2 w



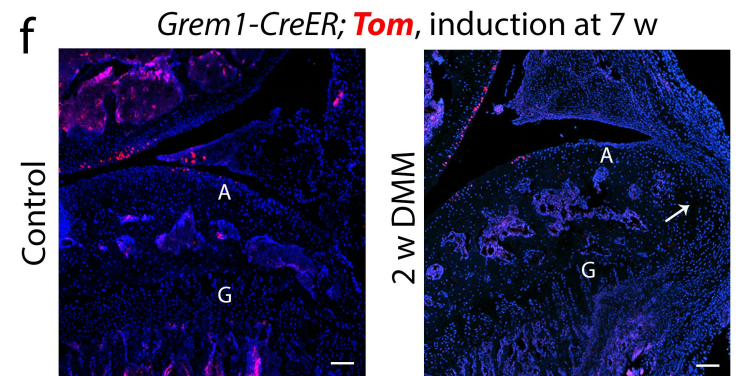
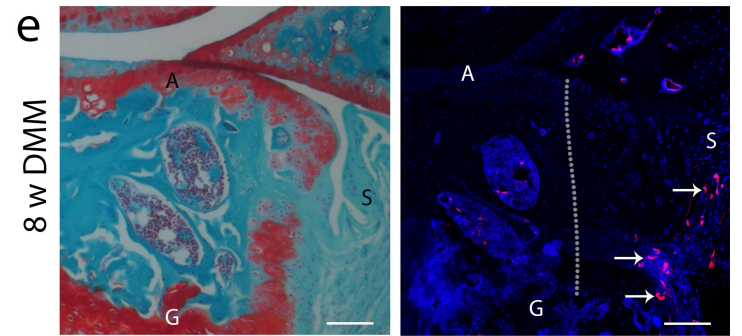
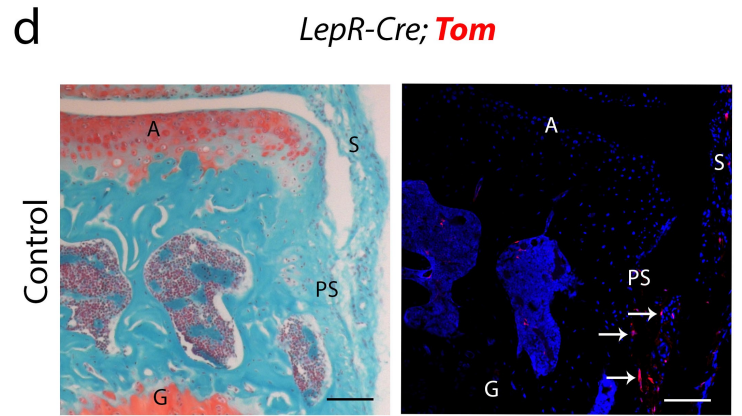
**d** *Col2-CreER; Tom*, induction at 2w

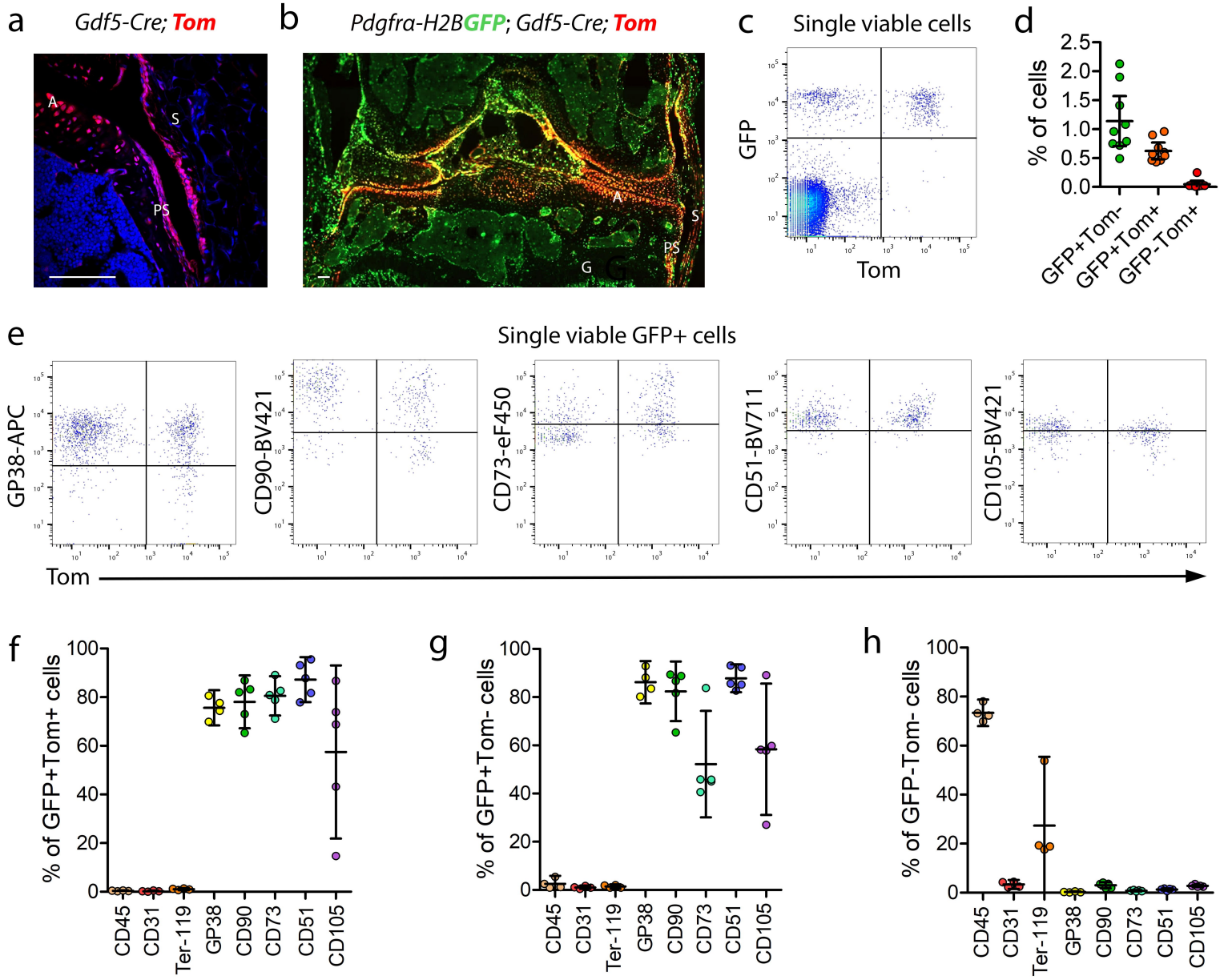


*Nes-GFP; Nestin-CreER; Tom*  
neonatal induction

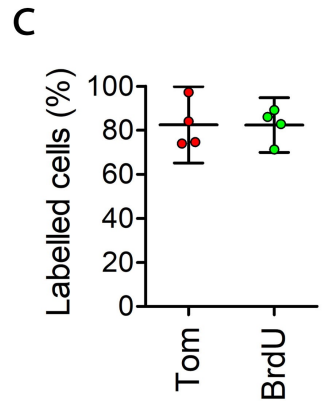
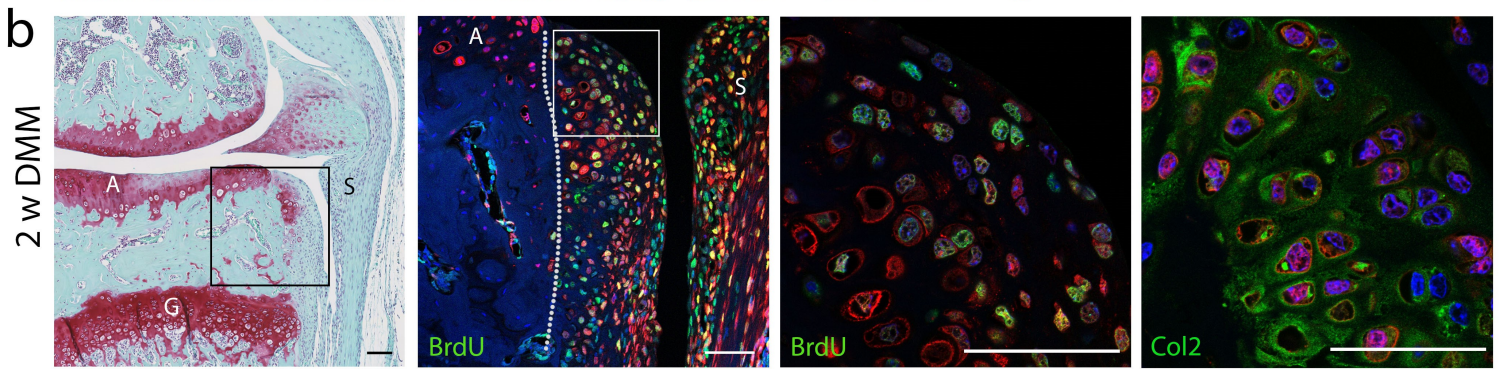
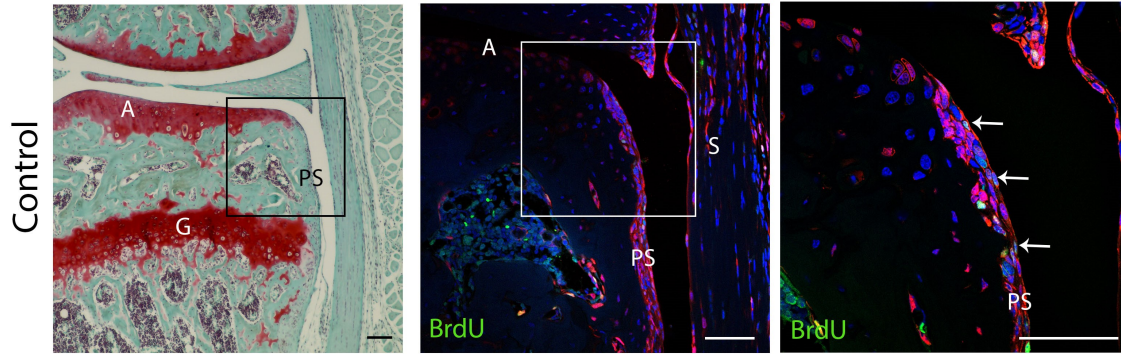


*LepR-Cre; Tom*

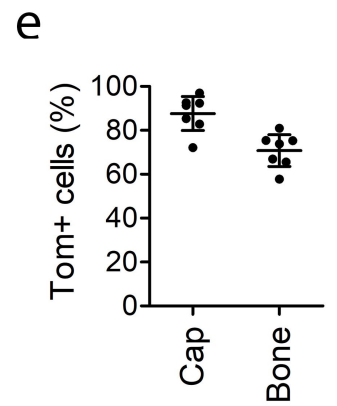
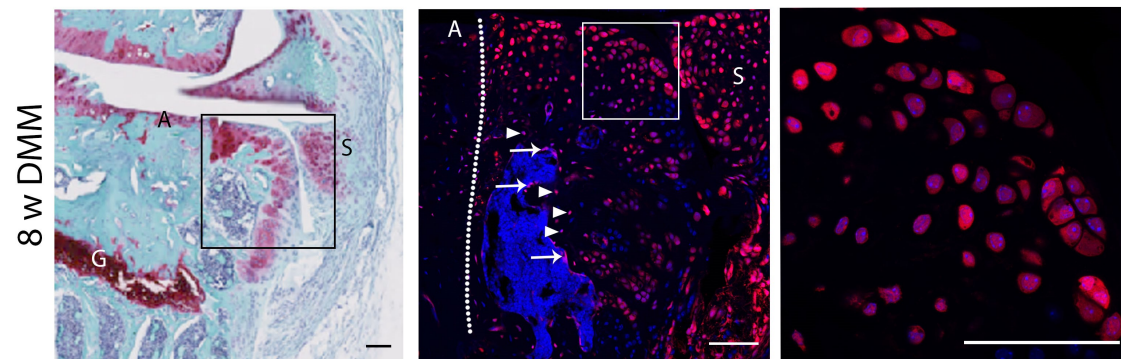




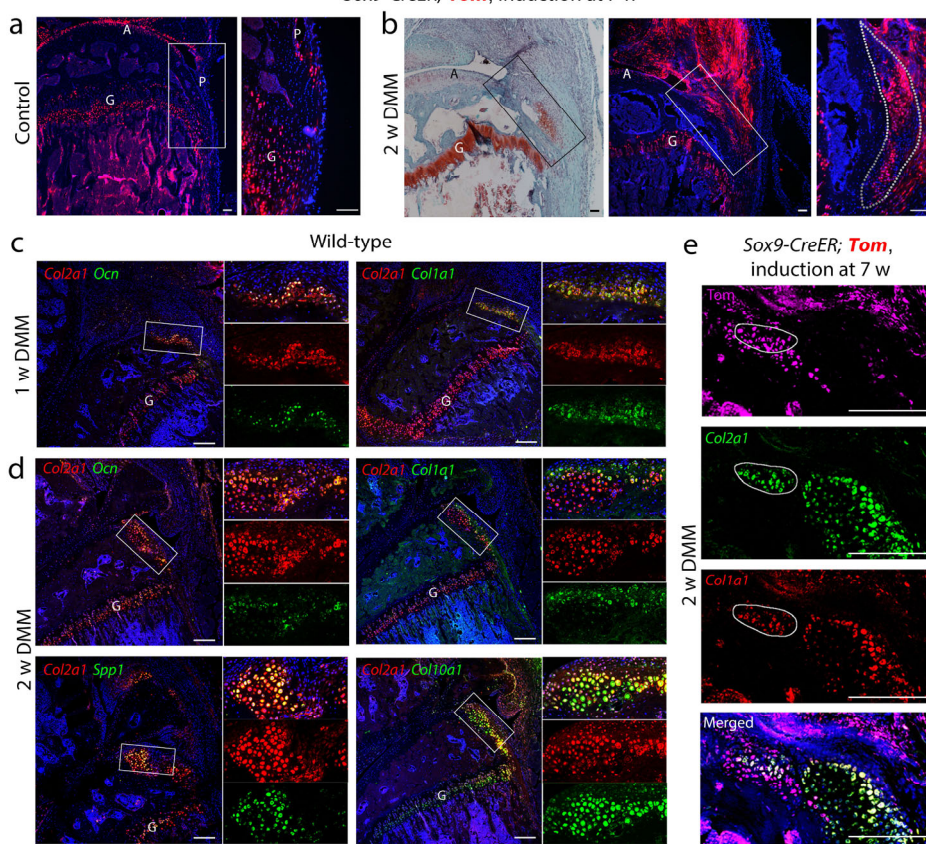
**a** *Gdf5-Cre; Tom, BrdU* for 2 w after DMM



**d** *Gdf5-Cre; Tom*

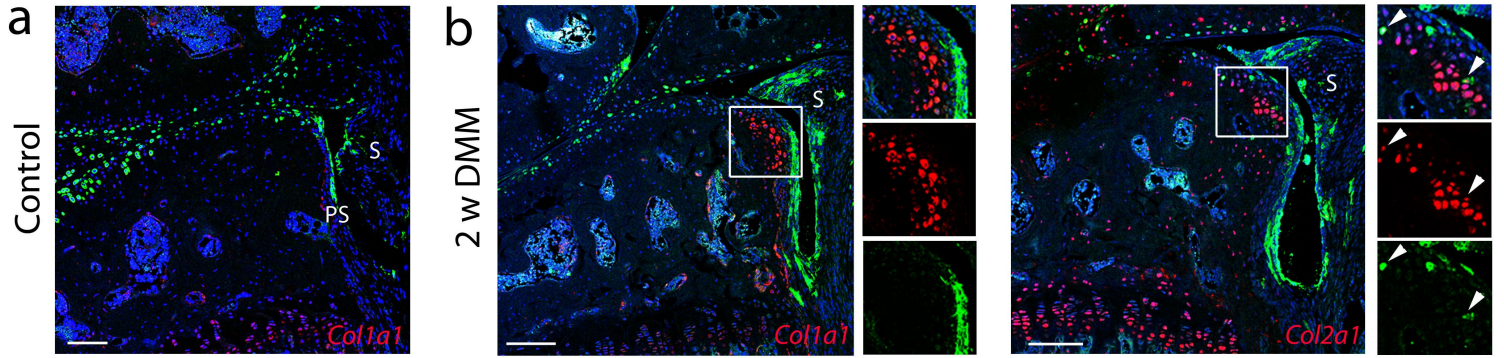


*Sox9-CreER*; **Tom**, induction at 7 w

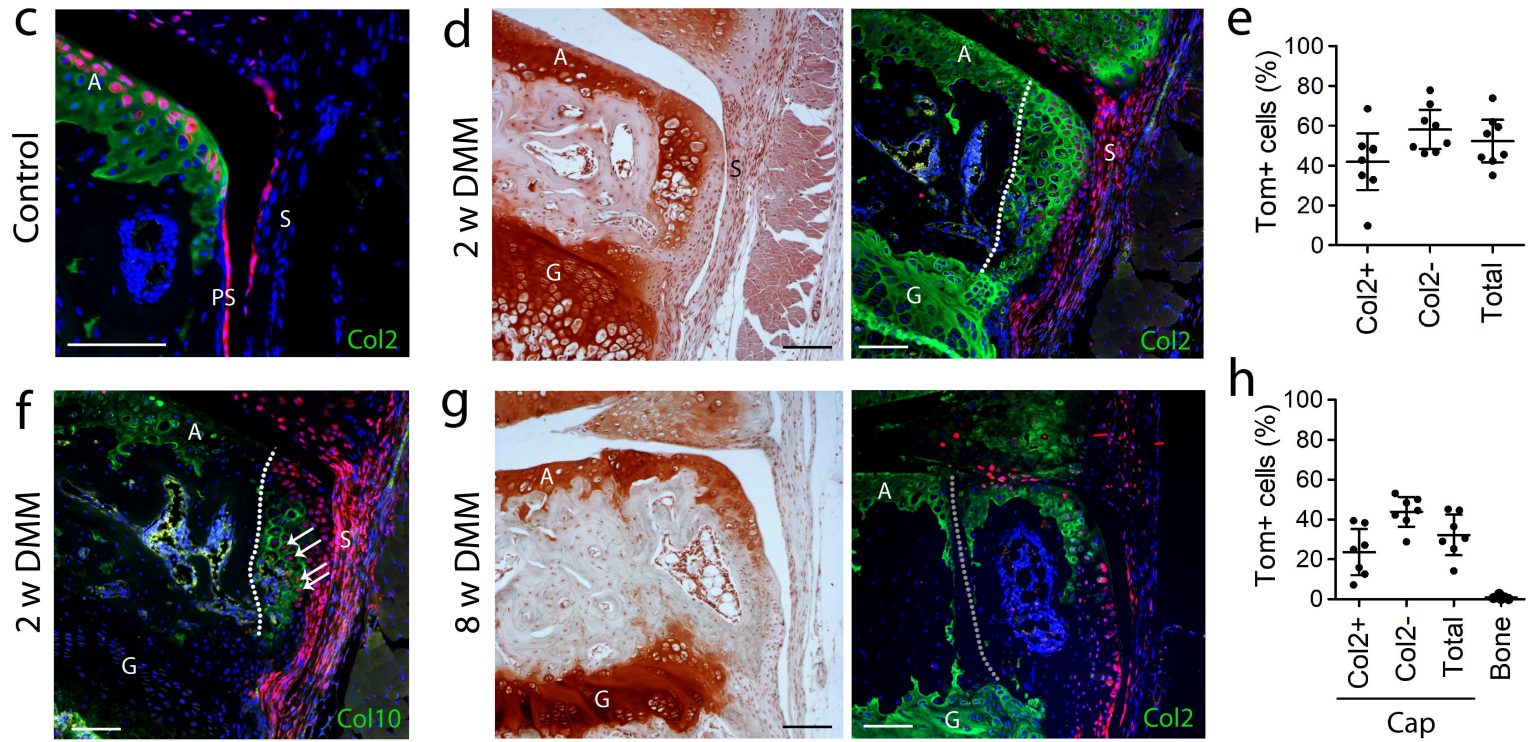




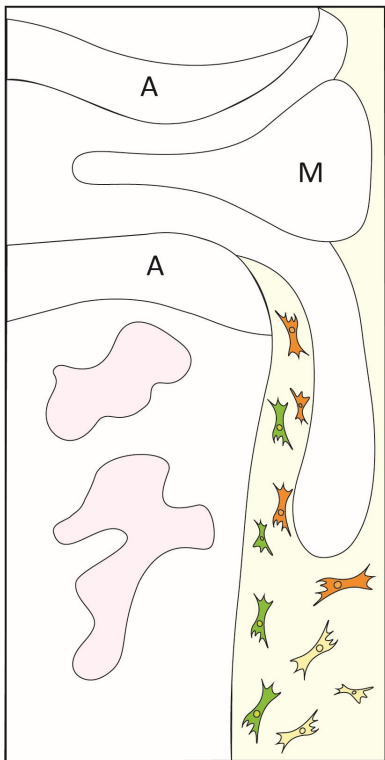
*Prg4-CreER; mTmG*, induction at 7 w



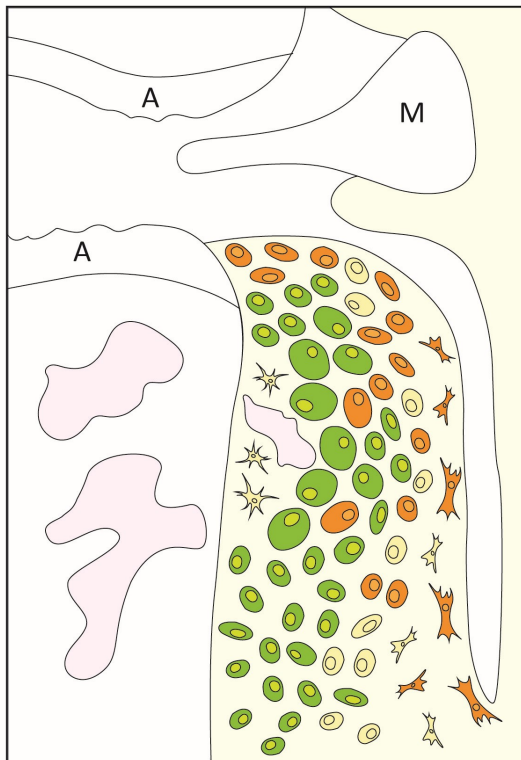
*Prg4-CreER; Tom*, induction at 8 w









normal

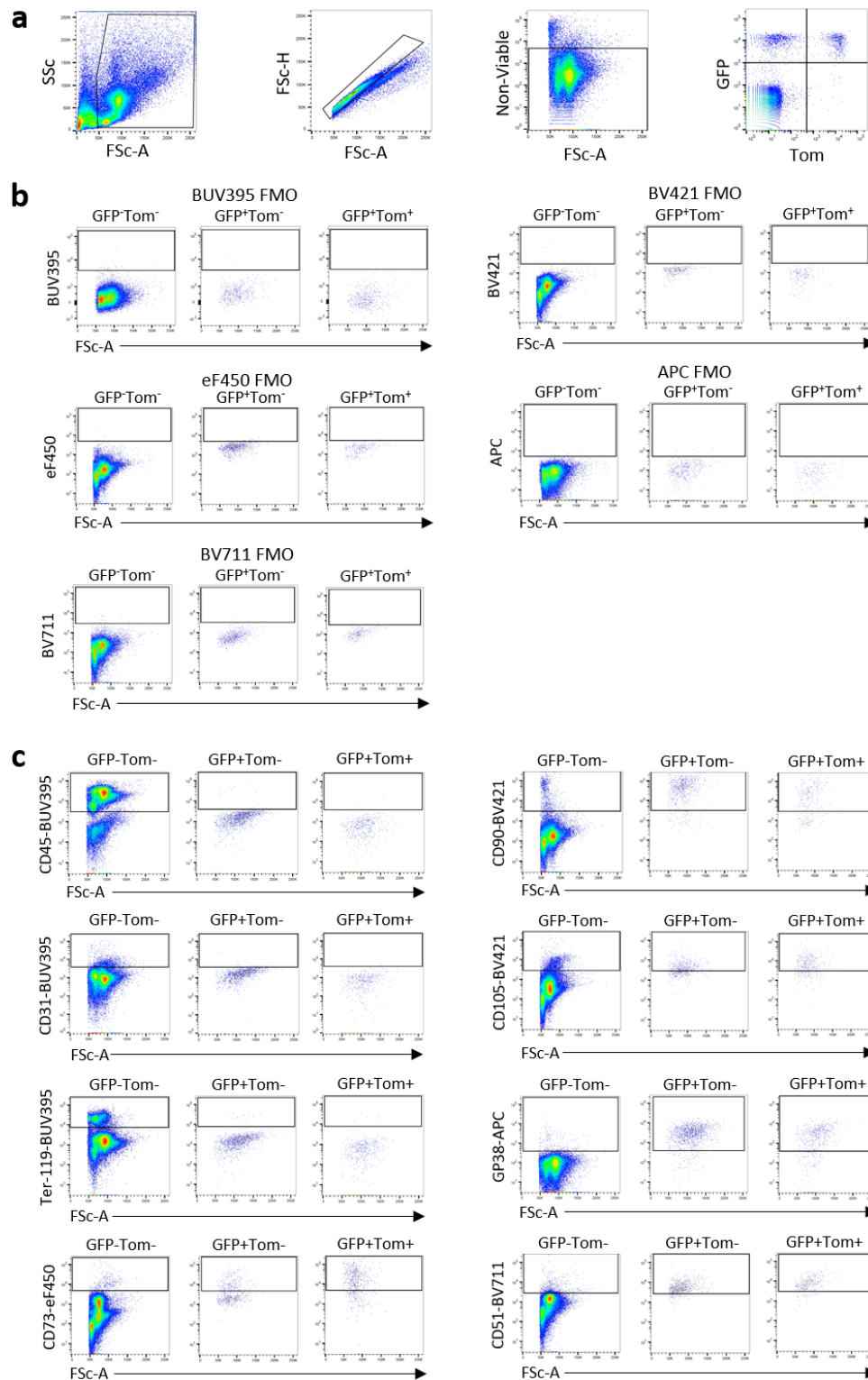


OA

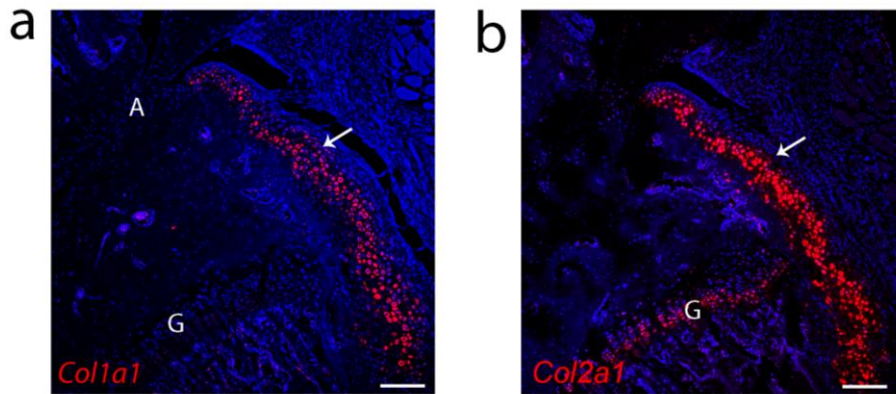


-  progenitors
-  chondrocytes/  
hybrid skeletal cells
-  osteocytes

-  Gdf5-lineage cells
  -  Prg4-lineage subset
  -  Sox9-lineage subset



**Supplementary Figure 1. Flow cytometry analysis of adult *Gdf5*-lineage and *Pdgfra*-expressing cells.** (a) Gating strategy to identify GFP-Tom<sup>-</sup>, GFP<sup>+</sup>Tom<sup>-</sup> and GFP<sup>+</sup>Tom<sup>+</sup> cells within single live cells freshly isolated from knees of adult *Pdgfra*-H2BGFP; *Gdf5*-Cre; *Tom* mice (n=9, 3 experiments). Erythrocytes and debris were gated out based on Forward and Side Scatter profile. Doublets and aggregates were excluded based on Forward Scatter parameters. Dead cells were excluded based on viability dye staining. (b) Gates for detection of cell surface markers were set using fluorescence-minus-one (FMO) controls. (c) Representative flow cytometry plots for the analysis of cell surface markers (n=4-5 for each marker, pooled data from 3 experiments).



**Supplementary Figure 2. Hybrid cells in early osteophytes of *Col2-CreER* animals.** Detection of *Col1a1* (a) and *Col2a1* (b) in early osteophyte (arrow) at 1 week post-DMM by fluorescence *in situ* hybridisations on adjacent sections of knee from 9-week-old *Col2-CreER; mTmG* mouse (n=2). Note also expression of *Col2a1* but not *Col1a1* in chondrocytes within the tibial growth plate (G). Nuclear counterstain is shown in blue. A: Articular cartilage. Scale bar indicates 100  $\mu$ m.

**Supplementary Table 1. Transgenic mouse lines.**

Short name	Full name	Source	Ref.
<i>Pdgfra-H2BGFP</i>	B6.129S4- <i>Pdgfratm11(EGFP)Sor/J</i>	JAX, stock no. 7669	1
<i>Nes-GFP</i>	Tg( <i>Nes-EGFP</i> )33Enik	G Enikolopov (CSHL)	2
<i>Col2-CreER</i>	FVB-Tg( <i>Col2a1-cre/ERT</i> )KA3Smac/J	JAX, stock no. 6774	3
<i>Pdgfra-CreER</i>	B6N.Cg-Tg( <i>Pdgfra-cre/ERT</i> )467Dbe/J	JAX, stock no. 18280	4
<i>Nes-CreER</i>	Tg( <i>Nes-cre/ERT2</i> )1Fsh	G Fishell (New York)	5
<i>LepR-Cre</i>	<i>Lep<sup>rtm3(cre)</sup>Mgmj</i>	L Heisler (Aberdeen)	6
<i>Grem1-CreER</i>	B6.Cg-Tg( <i>Grem1-cre/ERT</i> )3Tcw/J	JAX, stock no. 27039	7
<i>Gdf5-Cre</i>	Tg( <i>Gdf5-cre-ALPP</i> )1Kng	D Kingsley (Stanford)	8
<i>Prg4-CreER</i>	STOCK <i>Prg4<sup>tm1(GFP/cre/ERT2)</sup>Abl/J</i>	A Lassar (Harvard)	9
<i>Sox9-CreER</i>	<i>Sox9<sup>tm1(cre/ERT2)</sup>Haak</i>	H Akiyama (Kyoto)	10
<i>TdTomato</i>	B6.Cg-Gt(ROSA)26Sortm14( <i>CAG-tdTomato</i> )Hze/J	JAX, stock no. 6774	11
<i>TdTomato</i> (for Sox9-tracing)	B6;129S6-Gt(ROSA)26Sortm9( <i>CAG-tdTomato</i> )Hze/J	JAX, stock no. 7905	11
<i>Confetti</i>	STOCK Gt(ROSA)26Sortm1( <i>CAG-Brainbow2.1</i> )Cle/J	JAX, stock no. 13731	12
<i>mTmG</i>	B6.129(Cg)-Gt(ROSA)26Sortm4( <i>ACTB-tdTomato,-EGFP</i> )Luo/J	JAX, stock no. 7676	13

**Supplementary Table 2. Tamoxifen administration and age at surgery.**

Short name	Age at start	Dose, route and frequency of tamoxifen	Age at surgery
<i>Col2-CreER;Tom</i>	2 w	75 mg/kg i.p. daily for 5 days	13-14 weeks
<i>Pdgfra-CreER;</i> <i>Confetti</i>	11-12 w	200 mg/kg via oral gavage daily for 5 days, and 9 days later for a further 5 days	15-16 weeks (6 days after last Tam)
<i>Nes-CreER;Tom</i>	1 d	143 mg/kg via oral gavage to mother on day 1, 3, and 5 after delivery	10 weeks
<i>Grem1-CreER;Tom</i>	7 w	2 mg i.p. daily for 3 days	8 weeks (4 days after last Tam)
<i>Sox9-CreER;Tom</i>	7 w	2 mg i.p. daily for 3 days	8 weeks (4 days after last Tam)
<i>Prg4-CreER;mTmG</i>	7 w	2 mg i.p. every other day for 10 days	9 weeks (4 days after last Tam)
<i>Prg4-CreER;Tom</i>	8 w	75 mg/kg i.p. daily for 5 days, and 2 days later for a further 5 days	10 weeks (4 days after last Tam)

**Supplementary Table 3. Antibodies for immunohistochemistry.**

<b>Antibody</b>	<b>Clone</b>	<b>Manufacturer</b>	<b>Cat. No.</b>	<b>Conjugation</b>
Collagen type II (Col2)	polyclonal	Abcam	ab21291	unconjugated
Collagen type II (Col2)	polyclonal	Abcam	ab34712	unconjugated
Collagen type II (Col2)	6B3	Merck	MAB8887	unconjugated
Collagen type X (Col10)	X53	Quartett Berlin	1-CO097-05	unconjugated
BrdU	BU1/75 (ICR1)	Abcam	ab6326	unconjugated
mCherry (detects Tom)	polyclonal	Abcam	ab0081	unconjugated
mCherry (detects Tom)	polyclonal	Novus Biologicals	NBP2-25158SS	unconjugated
RFP (detects Tom)	polyclonal	Origene	AB1140-100	unconjugated
GFP	polyclonal	Abcam	ab6556	unconjugated
GFP	polyclonal	Abcam	Ab13970	unconjugated
GFP	polyclonal	Torrey Pines	TP401	unconjugated
Goat anti-chicken	polyclonal	Abcam	Ab150169	Alexa Fluor 488
Goat-anti-chicken	polyclonal	Abcam	Ab175477	Alexa Fluor 568
Donkey anti-goat	polyclonal	Abcam	Ab150129	Alexa Fluor 488
Donkey anti-goat	polyclonal	Thermo Fisher	A-21432	Alexa Fluor 555
Donkey anti-goat	polyclonal	Abcam	Ab150132	Alexa Fluor 594
Donkey anti-goat	polyclonal	Abcam	Ab150131	Alexa Fluor 647
Donkey anti-mouse	polyclonal	Thermo Fisher	A-21202	Alexa Fluor 488
Donkey anti-rabbit	polyclonal	Abcam	Ab150073	Alexa Fluor 488
Donkey anti-rabbit	polyclonal	Abcam	Ab150076	Alexa Fluor 594
Donkey anti-rabbit	polyclonal	Abcam	Ab150075	Alexa Fluor 647
Goat-anti-rabbit	polyclonal	Thermo Fisher	A-11011	Alexa Fluor 568

**Supplementary Table 4. Antibodies for flow cytometry.**

<b>Antibody</b>	<b>Clone</b>	<b>Manufacturer</b>	<b>Cat. No.</b>	<b>Conjugation</b>
CD73	TY/11.8	eBioscience	48-0731-82	eF450
CD90	OX-7	BD Biosciences	563770	BV421
CD105	MJ7/18	BD Biosciences	562760	BV421
CD51	RMV-7	BD Biosciences	740755	BV711
CD45	30-F11	BD Biosciences	564279	BUV395
CD31	390	BD Biosciences	740239	BUV395
Ter-119	TER-119	BD Biosciences	563827	BUV395
GP38	8.1.1	Biolegend	127410	APC
Viability Dye	-	eBioscience	65-0865-18	eF780

## References

1. Hamilton, T. G., Klinghoffer, R. A., Corrin, P. D. & Soriano, P. Evolutionary divergence of platelet-derived growth factor alpha receptor signaling mechanisms. *Mol. Cell. Biol.* **23**, 4013–25 (2003).
2. Mignone, J. L., Kukekov, V., Chiang, A. S., Steindler, D. & Enikolopov, G. Neural stem and progenitor cells in nestin-GFP transgenic mice. *J. Comp. Neurol.* **469**, 311–324 (2004).
3. Nakamura, E., Nguyen, M.-T. & Mackem, S. Kinetics of tamoxifen-regulated Cre activity in mice using a cartilage-specific CreER(T) to assay temporal activity windows along the proximodistal limb skeleton. *Dev. Dyn.* **235**, 2603–12 (2006).
4. Kang, S. H., Fukaya, M., Yang, J. K., Rothstein, J. D. & Bergles, D. E. NG2+ CNS glial progenitors remain committed to the oligodendrocyte lineage in postnatal life and following neurodegeneration. *Neuron* **68**, 668–81 (2010).
5. Balordi, F. & Fishell, G. Mosaic Removal of Hedgehog Signaling in the Adult SVZ Reveals That the Residual Wild-Type Stem Cells Have a Limited Capacity for Self-Renewal. *J. Neurosci.* **27**, 14248–14259 (2007).
6. Leshan, R. L., Björnholm, M., Münzberg, H. & Myers, M. G. Leptin Receptor Signaling and Action in the Central Nervous System. *Obesity* **14**, 208S-212S (2006).
7. Worthley, D. L. *et al.* Gremlin 1 Identifies a Skeletal Stem Cell with Bone, Cartilage, and Reticular Stromal Potential. *Cell* **160**, 269–284 (2015).
8. Rountree, R. B. *et al.* BMP Receptor Signaling Is Required for Postnatal Maintenance of Articular Cartilage. *PLoS Biol.* **2**, e355 (2004).
9. Kozhemyakina, E. *et al.* Identification of a Prg4-expressing articular cartilage progenitor cell population in mice. *Arthritis Rheumatol. (Hoboken, N.J.)* **67**, 1261–73 (2015).
10. Soeda, T. *et al.* Sox9-expressing precursors are the cellular origin of the cruciate ligament of the knee joint and the limb tendons. *Genesis* **48**, 635–44 (2010).
11. Madisen, L. *et al.* A robust and high-throughput Cre reporting and characterization system for the whole mouse brain. *Nat. Neurosci.* **13**, 133–140 (2010).
12. Snippert, H. J. *et al.* Intestinal Crypt Homeostasis Results from Neutral Competition between Symmetrically Dividing Lgr5 Stem Cells. *Cell* **143**, 134–144 (2010).
13. Muzumdar, M. D., Tasic, B., Miyamichi, K., Li, L. & Luo, L. A global double-fluorescent Cre reporter mouse. *Genesis* **45**, 593–605 (2007).